

# INVESTIGATION OF OPTIMIZATION OF DIELECTRIC TERAHERTZ ACCELERATION STRUCTURES

A. E. Gabriel<sup>†1</sup>, E. A. Nanni, SLAC National Accelerator Laboratory, Menlo Park, USA  
<sup>1</sup>also at University of California Santa Cruz, Santa Cruz, USA

## Abstract

THz-frequency accelerating structures could provide the accelerating gradients needed for next generation particle accelerators with compact, GV/m-scale devices. Current THz accelerators are limited by significant losses during transport of THz radiation from the generating nonlinear crystal to the electron acceleration structure. In addition, the spectral properties of high-field THz sources make it difficult to couple THz radiation into accelerating structures. Dielectric accelerator structures reduce these losses because THz radiation can be coupled laterally into the structure, as opposed to metallic structures where THz radiation must be coupled along the beam path. In order to utilize these advantages, we are investigating the optimization of THz accelerating structures for comparison between metallic and dielectric devices. These results will help to inform future designs of improved dielectric THz acceleration structures.

## INTRODUCTION

The THz frequency range holds many advantages for particle accelerators. Surface fields and shunt impedance in metallic structures scale as  $f^{1/2}$ . Because of this, accelerator operation at THz frequencies allows for extremely high fields and shunt impedance. Moving to THz frequencies also allows for more efficient structures that can operate at increased repetition rates with low emittance and high brightness beams.

There have been several successful demonstrations of THz acceleration using single cycle sources. So far, all THz accelerators have been composed of basic dielectric and metallic accelerating structures, and THz is coupled in to these structures along the beam path. Notably Xu *et al.*, recently demonstrated a novel cascaded accelerating scheme that uses two electron bunches and a copper accelerating structure with a quartz capillary [1]. In another demonstration Hibberd and colleagues were the first to accelerate high-charge fully relativistic electron bunches with THz pulses using a copper structure with a fused quartz lining [2]. These demonstrations show that THz accelerators have significant potential to greatly increase the capabilities of particle accelerators with smaller and more efficient accelerator structures.

Despite these recent achievements there are several challenges associated with THz acceleration. The spectral properties of high field THz sources make coupling into the accelerator structures difficult. In addition THz

transport from the generating crystal to the accelerating structure results in significant beam losses. Dielectric accelerators reduce these losses because THz radiation can be coupled laterally into the structure instead of along the beam path. In addition, Ohmic losses are significantly reduced in dielectric materials. Advanced fabrication methods such as femtosecond laser microfabrication allows for dielectric accelerators to have complex non-traditional geometries that can be optimized using simulation and optimization tools. In order to investigate the geometry optimization of dielectric THz accelerator structures several simulations were carried out and the resulting EM fields were analyzed. In addition, preliminary work has been conducted to investigate the simulation of THz generation via optical rectification in LiNbO<sub>3</sub> (LN). Obtaining an accurate simulation model of THz generation and the THz near field will improve and inform future dielectric THz accelerator designs and optimization. Progress on these efforts and the current status of the simulation work are presented here.

## PRELIMINARY SIMULATIONS

All simulations were carried out using an electromagnetic simulation and automatic differentiation package called Ceviche [3, 4]. Ceviche provides finite-difference frequency-domain (FDFD) and finite-difference time-domain (FDTD) electromagnetic simulation tools for solving Maxwell's equations. The program also provides methods for controlling minimum feature size allowing structures to be designed within manufacturing constraints. Optimization tools within the package were used to iteratively optimize the structure geometry to maximize the accelerating gradient.

### *Dielectric Accelerator*

FDFD Simulations of a single period of a dielectric accelerator were conducted using a 94 GHz continuous wave source incident from the left side of structure. The accelerator structure was optimized to maximize the accelerating gradient. All boundaries are perfectly matched absorbing layers (PML's). Calculation of the shunt impedance of this structure yielded a value of  $9.98 \times 10^5 \Omega/\text{m}$ . Simulation results of the optimized structure geometry and resulting electric fields are shown in Figs. 1 and 2.

<sup>†</sup> angabrie@slac.stanford.edu

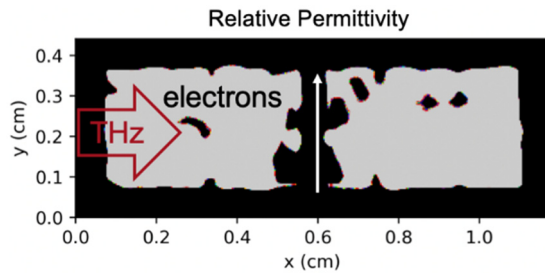


Figure 1: Final optimized geometry of single period dielectric accelerator structure. Grey regions are dielectric material ( $\epsilon_r = 9$ ), black regions are vacuum ( $\epsilon_r = 1$ ).

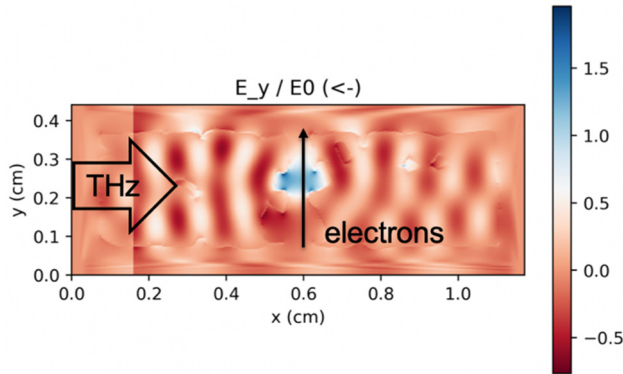


Figure 2: Electric fields produced by geometry in Fig. 1 by a 94 GHz continuous wave source incident from the left.

### Half LiNbO<sub>3</sub> Half Silicon

In addition to the results in Figs. 1 and 2 simulations of a half LN half silicon (Si) accelerator were carried out. In these simulations a 0.5 THz continuous wave source incident from the left was used and 5 periods were simulated. A periodic boundary condition was used. Calculation of the shunt impedance of this structure yielded a value of  $7.15 \times 10^7 \Omega/\text{m}$ . Simulation results of the optimized structure geometry and resulting electric fields are shown in Figs. 3 and 4.

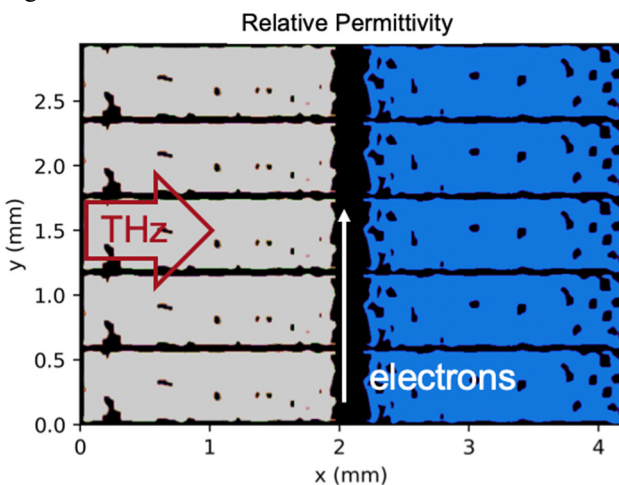


Figure 3: Final optimized geometry of a 5-period dielectric accelerator structure. Grey regions are LN ( $\epsilon_r = 42.5$ ), blue regions are silicon ( $\epsilon_r = 11.7$ ), and black regions are air ( $\epsilon_r = 1.0$ ). Permittivity in LN at THz frequencies from [5].

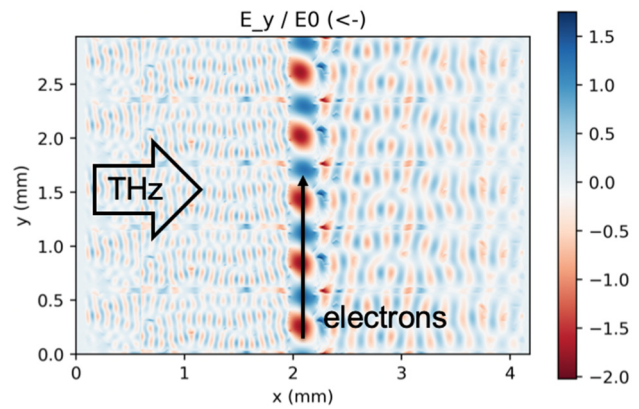


Figure 4: Electric fields produced by the structures in Fig. 3 by a 0.5 THz continuous wave source incident from the left.

The preliminary results in Figs. 1-4 show the potential of future manufacturable dielectric accelerator structures, motivating further investigation. Future simulations will be carried out using THz pulses, but a better understanding of THz generation and the THz near-field radiation are necessary first.

### THz Generation

Accurate simulation and modeling of the THz near field and THz generation process will improve and inform dielectric THz accelerator designs and optimization. Preliminary time-domain simulations have been carried out as a first attempt at simulating THz generation via optical rectification in a LN crystal. In these simulations an 800 nm laser pulse with a peak energy of 20 mJ and a time duration of 30 fs was used. The propagation of the laser pulse through a telescoping lens set up was calculated using the theory in [6]. The resulting laser pulse was then input as a plane source on the surface of the LN crystal to drive the FDTD simulation. The geometry of the initial set up is shown in Fig. 5. The size of the LN crystal was reduced so that the diagonal face was only slightly larger than the input laser pulse as seen in Fig. 6. This reduced the computational region and time that the simulation would take to complete. The source radiates in both directions coupling into and reflection off of the LN crystal, as shown in Fig. 7. Only the fields within the LN crystal are relevant for THz generation calculations. The simulation calculated the propagation of the fields forward in time for  $9.63 \times 10^{-13}$  s with  $\lambda/4$  spatial resolution. Simulations were run without nonlinearity in the LN refractive index, but future simulations will include this as well. Longer simulations that will track the complete path of the laser pulse through the LN crystal and show THz generation are currently in progress.

Content from this work may be used under the terms of the CC BY 3.0 licence (© 2021). Any distribution of this work must maintain attribution to the author(s), title of the work, publisher, and DOI

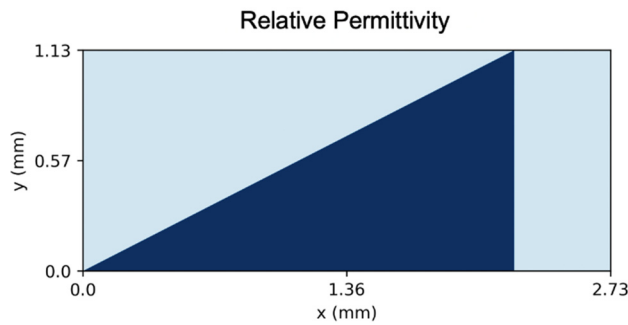


Figure 5: Simulation region showing LN crystal. Dark blue regions are LN ( $\epsilon_r = 5.0$ ) and light blue regions are air ( $\epsilon_r = 1$ ). Permittivity in LN for 800 nm from [7].

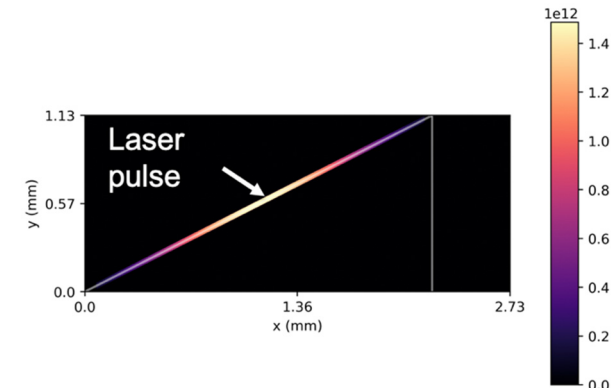


Figure 6: Positioning and field strength of input laser pulse as a plane source on the surface of the LN crystal in V/m. Grey outline indicates LN crystal geometry as show in Fig. 5.

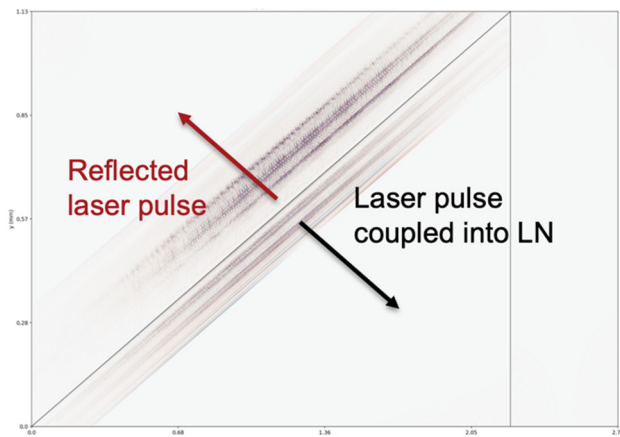


Figure 7: Preliminary simulation results showing  $\epsilon_r E$  after allowing the input laser pulse to propagate for  $9.63 \times 10^{-13}$  s. Grey outline indicates the border of the LN crystal.

These preliminary results show a first step towards simulating THz generation via optical rectification in LN and modelling the THz near field. Longer time domain simulations that will show the full propagation of the laser pulse through the LN crystal and the THz near field are currently in progress. Results from this investigation will be used to inform improved simulations of dielectric accelerator structures with THz pulses.

## CONCLUSION

We have presented preliminary simulation results showing optimized dielectric THz accelerators with manufacturable geometries and high shunt impedances. Preliminary simulations of THz generation are also included and show laser pulse propagation in an LN crystal with high spatial resolution. Future improved versions of these simulations will show the THz generation process and model the THz near field. These THz near field results will then be used to improve the dielectric accelerator simulations and optimization. These results show the first steps towards a highly optimized dielectric accelerator structure and motivate further investigation.

## ACKNOWLEDGEMENTS

The Authors would like to acknowledge E. C. Snively and M. A. K. Othman for helpful discussions. This work was supported by the Department of Energy Contract No. DE-AC02-76SF00515 (SLAC) and by NSF Grant No. PHY-1734015.

## REFERENCES

- [1] H. Xu *et al.*, “Cascaded high-gradient terahertz-driven acceleration of relativistic electron beams”, *Nat. Photonics*, 2021. doi:10.1038/s41566-021-00779-x
- [2] M. T. Hibberd *et al.*, “Acceleration of relativistic beams using laser-generated terahertz pulses”, *Nat. Photonics*, vol. 14, no. 12, pp. 755–759, 2020. doi:10.1038/s41566-020-0674-1
- [3] T. W. Hughes, I. A. D. Williamson, M. Minkov, and S. Fan, “Forward-mode differentiation of Maxwell’s equations”, *ACS Photonics*, vol. 6, no. 11, pp. 3010–3016, 2019. doi:10.1021/acsp Photonics.9b01238
- [4] GitHub, <https://github.com/fancompute/ceviche>
- [5] X. Wu, C. Zhou, W. R. Huang, F. Ahr, and F. X. Kärtner, “Temperature dependent refractive index and absorption coefficient of congruent lithium niobate crystals in the terahertz range”, *Opt. Express*, vol. 23, no. 23, p. 29729–29737, 2015. doi:10.1364/OE.23.029729
- [6] K. Ravi *et al.*, “Theory of terahertz generation by optical rectification using tilted-pulse-fronts”, *Opt. Express*, vol. 23, no. 4, p. 5253, 2015. doi:10.1364/OE.23.005253
- [7] O. Gayer, Z. Sacks, E. Galun, and A. Arie, “Temperature and wavelength dependent refractive index equations for MgO-doped congruent and stoichiometric LiNbO<sub>3</sub>”, *Appl. Phys. B*, vol. 91, no. 2, pp. 343–348, 2008. doi:10.1007/s00340-008-2998-2